Supplementary Information

Covalent Functionalization of Boron Nitride Nanosheets via Reductive Activation

Changjiu Sun,[a] Jian Zhao,[a,b,c,d*] Deli Zhang,[a] Hongge Guo,[b] Xin Wang,[a] and Haiqing Hu[a]

[a] Key Laboratory of Rubber-Plastics Ministry of Education/Shandong Provincial Key Laboratory of Rubber-Plastics, Qingdao University of Science & Technology, No. 53 Zhengzhou Road, Qingdao 266042, China and School of Materials Science and Engineering, Qilu University of Technology (Shandong Academy of Sciences), Jinan 250353, China

[b] Key Laboratory of Organosilicon Chemistry and Material Technology of Ministry of Education, Hangzhou Normal University, Hangzhou 311121, China

[c] State Key Laboratory of Molecular Engineering of Polymers (Fudan University), Shanghai 200433, China

[d] State Key Laboratory of Polymer Materials Engineering, Sichuan University, Chengdu 610065, China

AFM measurements of h-BN and solvent-exfoliated BNNSs

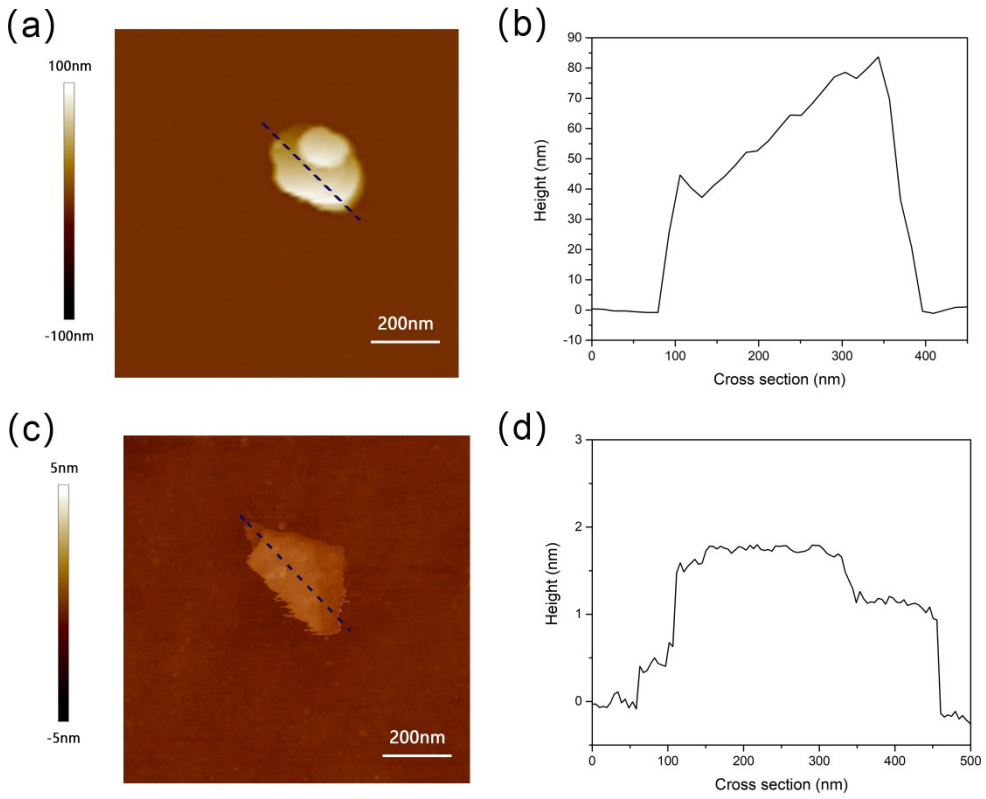

Fig. S1. (a) AFM image and (b) height curve of h-BN, (c) AFM image and (d) height curve of solvent-exfoliated BNNSs.

TEM image and electron diffraction pattern of solvent-exfoliated BNNSs

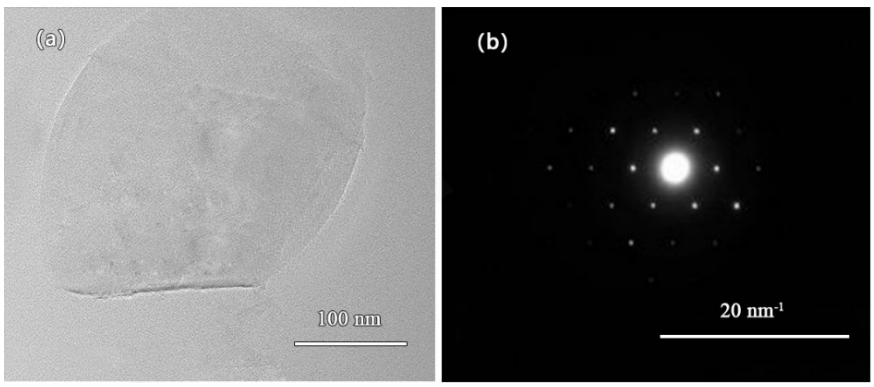

Fig. S2. (a)TEM image and (b) electron diffraction pattern of solvent-exfoliated BNNSs.

X-ray diffraction patterns of h-BN and solvent-exfoliated BNNSs

The x-ray diffraction peak positions of solvent-exfoliated BNNSs are approximately the same as those of the h-BN raw material,[1] in indicating favorable crystallinity of solvent-exfoliated BNNSs（Fig. S2）. Compared with the FWHM（0.305）of h-BN at the (002) crystal plane, the FWHM (1.210) of the diffraction peak of solvent-exfoliated BNNSs at the (002) plane becomes larger. That is, the thickness of the BNNSs is significantly reduced upon solvent exfoliation according to the Scherrer's formul.[2] The diffraction peak of the BNNSs on the (002) crystal face is observed at 26.55°, showing a shift to lower angle in comparison with h-BN. According to the Bragg's law, the crystalline spacing between nanosheets is increased. This behavior can be explained by the intercalation of solvent molecules trapped between the sheets during the exfoliation process. In addition, it is noticed that the peak intensity ratio I(004)/I(100) of BNNSs increases, indicating that the exfoliation of BNNSs proceeds along the (002) crystal face.

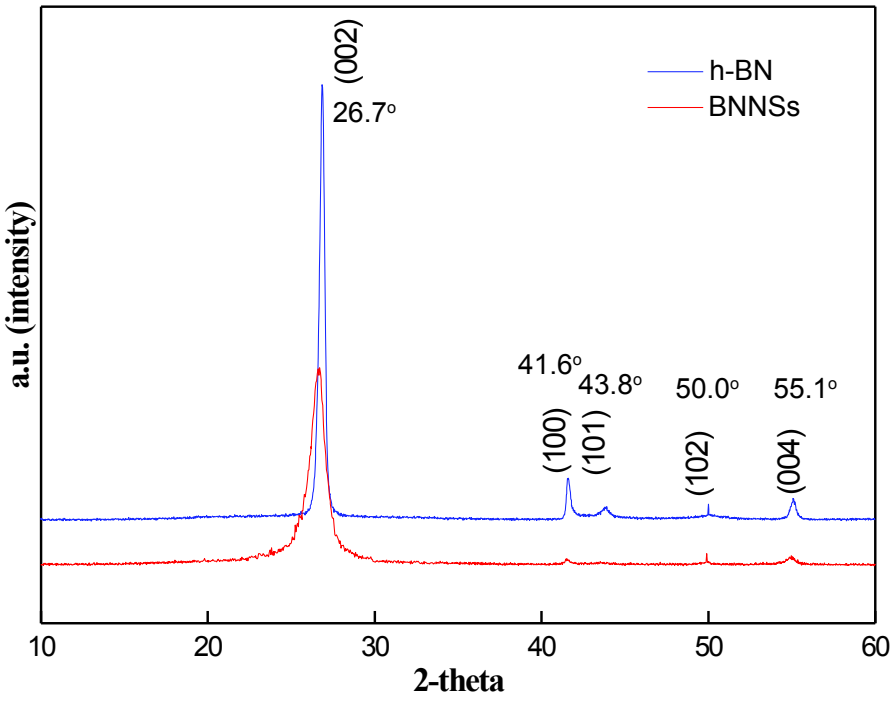

Fig. S3. X-ray diffraction patterns of h-BN and solvent-exfoliated BNNSs.

Nitrogen adsorption–desorption isotherm measurements

Brunauer–Emmett–Teller (BET) surface area of the original h-BN, solvent-exfoliated BNNSs and functionalized BNNSs ($C_{18}H_{37}$-BNNSs(Br)), was measured to be 25, 191 and 246 $m^2\ g^{-1}$, respectively. The increased specific surface area suggests that the number of BN layers is decreased.

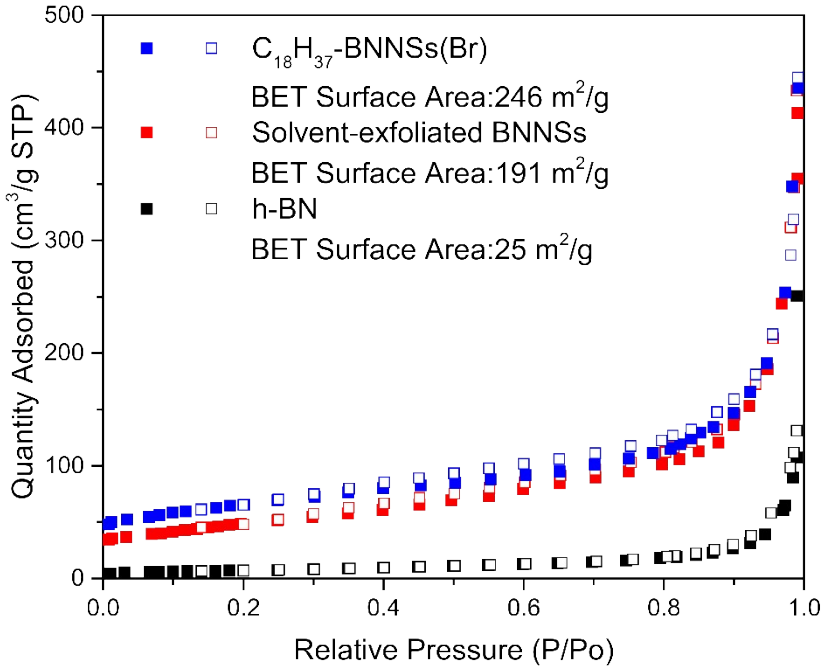

Fig. S4. Nitrogen adsorption and desorption isotherm and Brunauer–Emmett–Teller (BET) surface area of original h-BN, solvent-exfoliated BNNSs and $C_{18}H_{37}$-BNNSs(Br).

Zeta potentials measurements

The original h-BN shows a zeta potential of -12.4mV. A negative zeta potential indicates that the surface of h-BN mainly adsorbs negative ions in water due to the larger isoelectric point of water in comparison with BN.[3] The zeta potential of solvent-exfoliated BNNSs is reduced to -37.6 mV. The decrease in zeta potential indicates improved dispersion stability of BNNSs in water.[4, 5] After the alkyl modification, the zeta potential increases to -19.7 mV, which can be attributed to the enhancement of oil-wet behavior of BNNSs after functionalization.

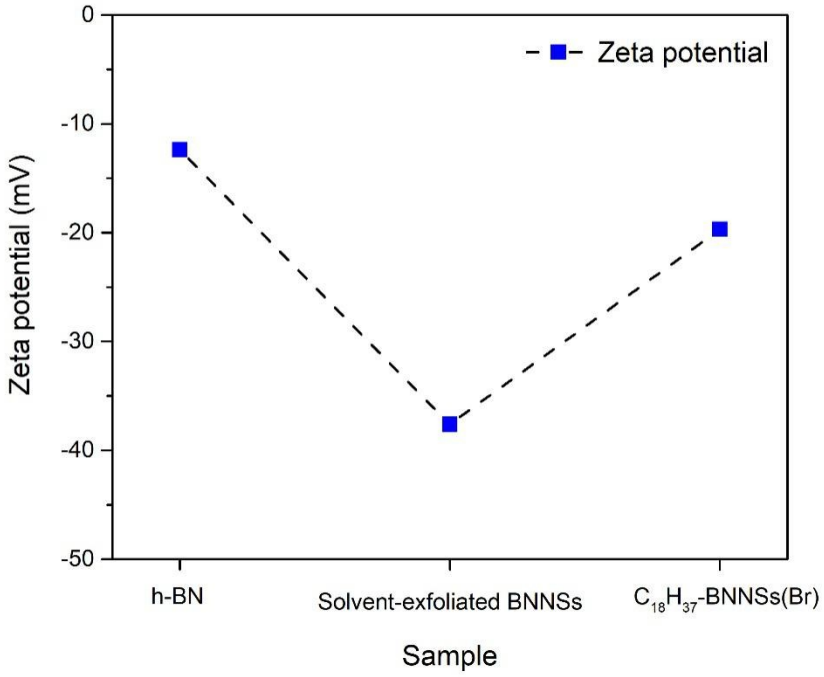

Fig. S5. Zeta potentials of h-BN, solvent-exfoliated BNNSs and $C_{18}H_{37}$-BNNSs(Br).

TEM images and electron diffraction patterns of different alkyl functionalized BNNSs

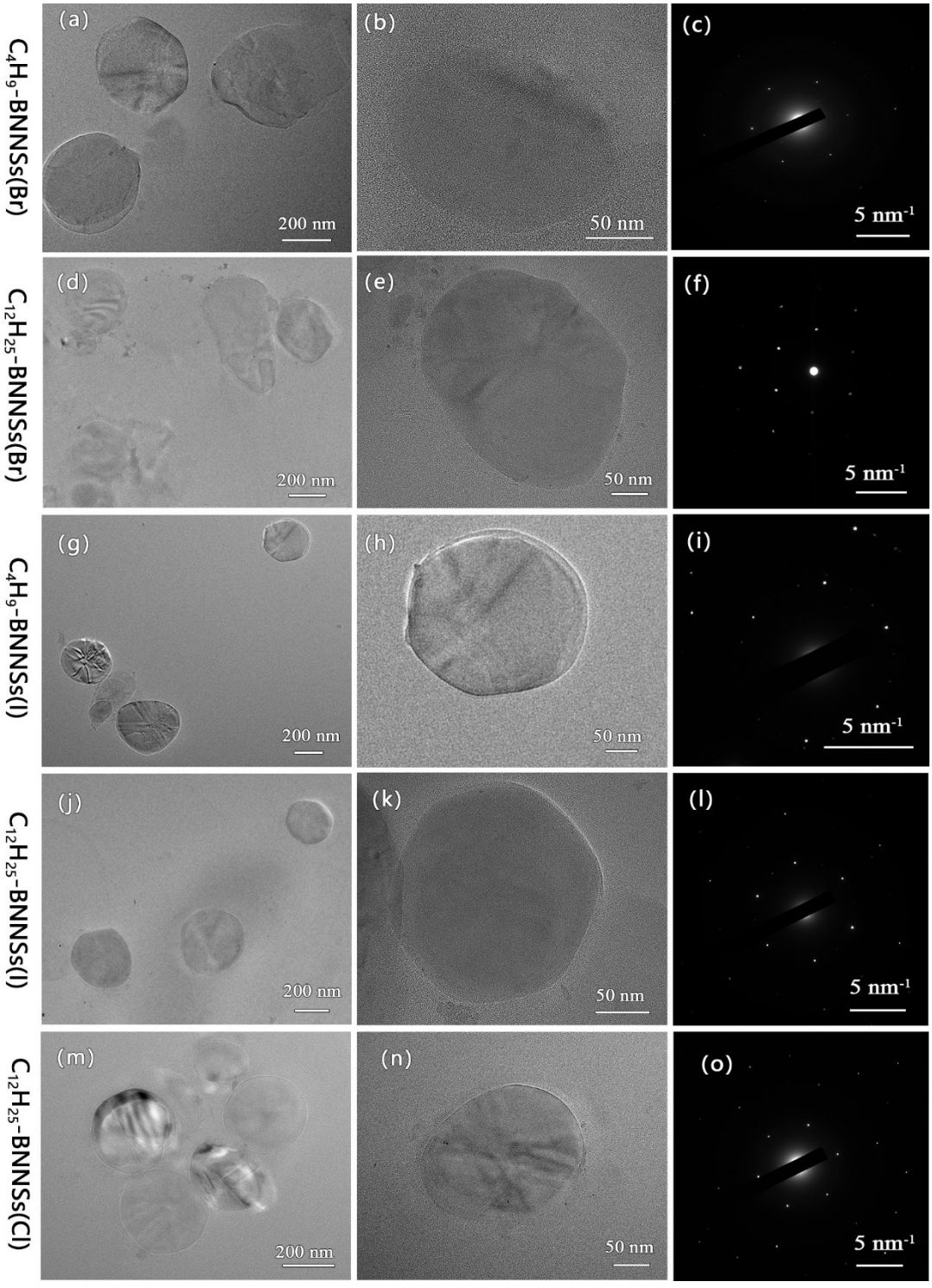

Fig. S6. The TEM images of different alkyl functionalized BNNSs and their electron diffraction pattern images.

DSC measurements of pure LDPE and LDPE/BNNSs nanocomposites

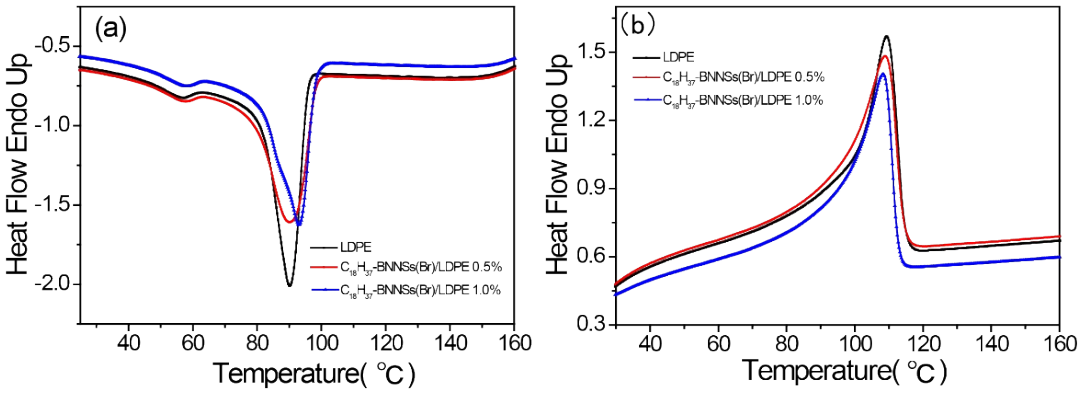

Fig. S7. DSC cooling (a) and second-run heating (b) curves of pure LDPE and LDPE/alkyl functionalized BNNSs nanocomposites（0.5 wt. % and 1.0 wt. %).

The crystallization and melting behaviors of pure LDPE and LDPE nanocomposites （0.5 wt. % and 1.0 wt. %) were investigated by DSC (Fig. S4), and the obtained melting peak temperature (T_m) in the second-run heating process is summarized in Table S3. Crystallinity X_c can be determined using the following formula:

$$X_c = \frac{\Delta H_f}{(1-\varphi)\ \Delta H^*} \times 100\% \qquad (1)$$

Where ΔH_f is the measured melting enthalpy of samples, ΔH^* is the melting enthalpy of the completely crystalline LDPE (277.1 J/g), and ϕ is the mass fraction of alkylated BNNSs in the LDPE-based nanocomposites.

The DSC cooling and second-run heating curves of pure LDPE and LDPE/alkylated BNNS nanocomposites are illustrated in Fig. S4. The pure LDPE, 0.5 wt. % and 1.0 wt. % nanocomposites exhibit a broad crystallization peak centered at 90.25 °C, 90.25 °C and 93 °C, respectively. No cold-crystallization peak is observed, indicating that LDPE has crystallized completely in the previous cooling process. All the samples exhibit a strong exothermic peak upon cooling from the melt and a broad melting peak. T_m of LDPE decreases slightly with the rise of filler content. Moreover, the melting enthalpy and

crystallinity also decrease as the filler content increases, indicating that the loading of the alkylated BNNSs does not contribute to LDPE crystallization.

Table S1. The atomic concentrations of solvent-exfoliated BNNSs and $C_{18}H_{37}$-BNNSs(Br)

Sample	B	N	C	O
BNNSs	47.01	48.42	1.02	3.35
$C_{18}H_{37}$-BNNSs(Br)	43.94	44.23	8.13	3.70

Table S2. The solubility data of solvent-exfoliated BNNSs and alkyl functionalized BNNSs in different organic solvents

Sample	Chloroform （mg/ml）	1,2-dichlorobenzene （mg/ml）
BNNSs	0.09	0.06
C_4H_9-BNNSs(Br)	0.14	0.10
$C_{12}H_{25}$-BNNSs(Br)	0.31	0.21
$C_{18}H_{37}$-BNNSs(Br)	0.46	0.33
C_4H_9-BNNSs(I)	0.17	0.12
$C_{12}H_{25}$-BNNSs(I)	0.36	0.23
$C_{12}H_{25}$-BNNSs(Cl)	0.22	0.16

Table S3. The results from the DSC curves for pure LDPE and LDPE/alkyl functionalized BNNSs nanocomposites.

Sample	LDPE	$C_{18}H_{37}$-BNNSs(Br) /LDPE-0.5%	$C_{18}H_{37}$-BNNSs(Br) /LDPE-1.0%
Tm (°C)	109.3	108.9	108.2
Xc (%)	36.9	36.0	34.6

Supplementary experimental section

XRD measurements of the BN samples were conducted using a D-MAX 2500/PC diffractometer (Bragg-Brentano geometry) equipped with a monochromatized Cu Kα radiation source (λ = 1.5406 Å) operating at a voltage of 40kV and current of 100mA.

Brunauer-Emmett-Teller (BET) surface areas of the BN samples were obtained from a nitrogen adsorption-desorption isotherm using an ASAP 2020 analyzer (Micromeritics Instrument Co.), and the outgassing process was run at 200 °C for 12 h.

Zeta potentials of the BN samples in aqueous suspension were measured with Zetasizer NANO-ZS90 (Malvern Instrument, UK). 2 mL of BN suspension was transferred into a measuring cell, and the measurement was run at V = 10 V and T = 25 ^{o}C with a switch time of t = 50 s.

Differential scanning calorimetry (DSC) measurements were carried out by using a DSC-204F1 from Netzsch (N_2 flow). The samples were heated from room temperature to 170 ^{o}C, maintained at this temperature for 5 min, then cooled to room temperature and heated again to 170 ^{o}C. The heating and cooling rates were set to 10 ^{o}C min^{-1} in all cases.

REFERENCES

1. M. Du, Y. Wu and X. Hao, *CrystEngComm*, 2013, **15**, 1782-1786.

2. R. Nemanich, S. Solin and R. M. Martin, *Physical Review B*, 1981, **23**, 6348.

3. K. Wattanakul, H. Manuspiya and N. Yanumet, *Colloids and Surfaces A: Physicochemical and Engineering Aspects*, 2010, **369**, 203-210.

4. I. M. Joni, R. Balgis, T. Ogi, T. Iwaki and K. Okuyama, *Colloids and Surfaces A: Physicochemical and Engineering Aspects*, 2011, **388**, 49-58.

5. J. Wang, H. Li, G. Li, Z. Liu, Q. Zhang, N. Wang and X. Qu, *Journal of Applied Polymer Science*, 2017, **134**.44987